



Zinc selective chemosensors based on the flexible dipicolylamine and quinoline

Hong Gyu Lee^a, Ju Hoon Lee^a, Seung Pyo Jang^{a,b}, In Hong Hwang^a, Sung-Jin Kim^c, Youngmee Kim^c, Cheal Kim^{a,*}, Roger G. Harrison^{b,*}

^a Department of Fine Chemistry, Seoul National University of Science & Technology, Seoul 139-743, Republic of Korea

^b Department of Chemistry and Biochemistry, Brigham Young University, Provo, UT, USA

^c Department of Chemistry and Nano Science, Ewha Womans University, Seoul 120-750, Republic of Korea

ARTICLE INFO

Article history:

Received 10 July 2012

Received in revised form 14 September 2012

2012

Accepted 17 September 2012

Available online 27 September 2012

Keywords:

Zinc sensor

Dipicolylamine

Fluorescence enhancement

ABSTRACT

Zinc sensor molecules containing quinoline have been synthesized, which show fluorescence in the presence of Zn²⁺. The nitrogen in quinoline is critical to fluorescence and fluorescence enhancement is promoted by deprotonating the sensor's amide. One of the sensors is highly selective for Zn²⁺ over Cd²⁺ and other cations such as Hg²⁺, Fe²⁺, Mn²⁺ and Ca²⁺. This selectivity can be attributed to the increased absorption of the sensor in the presence of Zn²⁺ and the strong binding of Zn²⁺. Structural studies, including X-ray and NMR, show the ability of dipicolylamine (DPA) to bind in facial and meridional manners to Zn²⁺. Crystal structures of different compounds show Zn²⁺ coordinating to three, four, and five nitrogens from the compounds. They also indicate that the selectivity of DPA containing compounds towards Zn²⁺ may originate from Zn²⁺ being stable in different coordination environments.

© 2012 Elsevier B.V. All rights reserved.

1. Introduction

Over the last several years research has steadily progressed on the synthesis of zinc sensors. Zinc ions are colorless in aqueous solutions, do not have unpaired electrons, and remain in the plus two oxidation state. It is thus difficult to image zinc ions and know their concentration in biological environments. However, it has been discovered that some unique molecules in the presence of Zn²⁺ fluoresce, which fluorescence can be monitored and quantified [1]. In fact, Zn²⁺ can now be imaged in cells and living organisms [2].

Zinc sensors often have two parts, a chelating group that binds zinc and an aromatic group that fluoresces when zinc is bound [3]. Dipicolylamine (DPA) is one molecule that has been used for the zinc binding group, it having three nitrogens for zinc chelation [4]. DPA has been bonded to many different fluorophores, including ones with amide linkages [5]. An important property of DPA which makes it especially good for binding Zn²⁺ is its flexibility. Zn²⁺ has 10 valence electrons in *d* orbitals, which provide no ligand field stabilization energy to be in an octahedral, tetrahedral, or other configuration. However, Zn²⁺ has a plus two charge and a relatively small radii for its nuclear charge. Taking these properties together means Zn²⁺ is a fairly strong Lewis acid with preference to bind nitrogen ligands and have stability in various geometries.

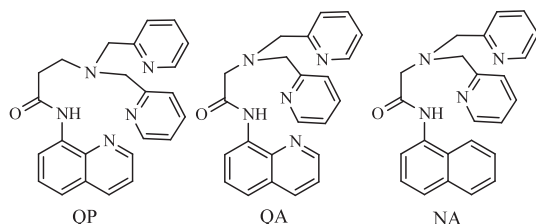
* Corresponding authors. Tel.: +82 2 970 6693; fax: +82 2 973 9149 (C. Kim), tel.: +1 801 422 8096; fax: +1 801 422 0153 (R.G. Harrison).

E-mail addresses: chealkim@seoultech.ac.kr (C. Kim), roger_harrison@byu.edu (R.G. Harrison).

These properties make it coordinate more strongly in different geometries than larger divalent cations such as Ca²⁺ and neighboring transition metal cations, such as Fe²⁺, that prefer a certain ligand geometry. This ability of Zn²⁺ to accommodate different geometries may even make it detectable in the presence of Cu²⁺. DPA has the flexibility to coordinate in meridional and facial arrangements, as well as others in between. Thus, DPA can accommodate Zn²⁺ in different geometries such as octahedral and trigonal bipyramidal.

Quinoline is still an important fluorophore for Zn²⁺ sensors and has been combined with DPA. The quinoline group was one of the first molecules used as a fluorophores for Zn²⁺ sensing [6]. Recently, Zn²⁺ has been shown to enhance fluorescence of quinoline molecules that contain amide amine ethers [7], hydroxyl quinolines [8], hydroxyl quinolines with amino rings [9], and spiropyran [10]. Combining DPA with quinoline has produced sensors with an array of properties such as femtomolar zinc detection [11], large Stokes shifts [12], fluorescence by two-photon [13], ratiometric detection of zinc [14], and multiple zinc binding sites [15].

We report the synthesis of the zinc sensor QP, which has a DPA subunit for Zn²⁺ coordination and a quinoline group for fluorescence (Scheme 1). We have intentionally increased the carbon chain length by one carbon between the fluorophore and zinc-binding domain in an attempt to change the fluorescence response to zinc. We also investigate zinc-binding molecules QA and NA, which are closely related to QP, but vary by a carbon atom between the binding and fluorescence domains (QA) or a nitrogen atom in



Scheme 1. Structures of Zn^{2+} binding compounds, QP, QA and NA.

the naphthyl ring (NA). Crystal structures of the molecules coordinated to Zn^{2+} show DPA coordinating in meridional and facial arrangements. Also, proton NMR data indicate the different DPA binding modes. We found that the quinoline-based sensors have intense fluorescence in the presence of zinc and fluoresce selectively for zinc over main group and transition metal ions.

2. Experimental

2.1. Materials and instruments

Reagents and solvents were purchased from commercial suppliers and used as received. QA was synthesized similar to a published procedure [16]. *Caution:* perchlorate salts are potentially explosive with organic ligands, handle them carefully. Absorption spectra were recorded at 25 °C using a Perkin Elmer model Lambda 2S UV–Vis spectrometer. A BIO RAD FTS 135 spectrometer was used for IR KBr pellets. 1H NMR measurements were performed on a Varian 400 MHz spectrometer and chemical shifts are recorded in ppm. Fluorescence measurements were performed on a Perkin Elmer model LS45 Fluorescence spectrometer. X-ray diffraction data were collected on a Bruker SMART AXS diffractometer. Electrospray ionization mass spectra (ESI-MS) were collected on a Thermo Finnigan (San Jose, CA, USA) LCQ™ Advantage MAX quadrupole ion trap instrument. Elemental analysis for carbon, nitrogen, and hydrogen was carried out by using a vario MACRO (Elemental Analysensysteme, Germany) in the Laboratory Center of Seoul National University of Science and Technology, Korea.

Energy calculations were done using SPARTAN 08 version 1.2.1 by Wavefunction, Inc.

2.2. Preparation of 3-chloro-*N*-(quinolin-8-yl)propanamide

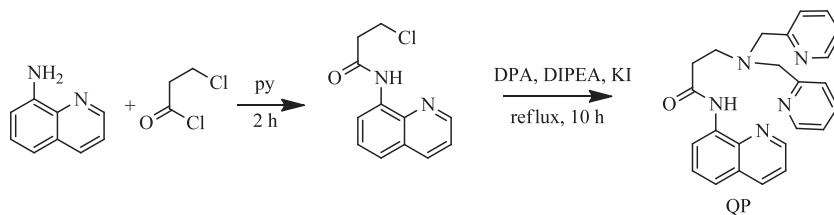
3-Chloropropionyl chloride (2.00 mL, 20.9 mmol) was dissolved in chloroform (10 mL), it was then added dropwise to a cooled and stirred solution of 8-aminoquinoline (0.740 g, 5.13 mmol) and pyridine (0.43 mL, 5.2 mmol) in chloroform (10 mL) over a period of 1 h. After the reaction solution was allowed to warm to room temperature, it was stirred for 2 h and the solvent was removed under reduced pressure to obtain an ivory powder, which was washed with dichloromethane and diethyl ether. Yield: 1.00 g (75.3%), 1H NMR (DMSO- d_6 , 400 MHz): δ 10.32 (NHCO, s, 1H), 8.94 (d, J = 4.0 Hz, 1H), 8.66 (d, J = 4.0 Hz, 1H), 8.41 (d, J = 8.0 Hz, 1H), 7.66 (t, J = 8.0 Hz, 1H), 7.62 (t, J = 8.0 Hz, 1H), 7.58 (d, J = 8.0 Hz, 1H) 3.94 (–CH $_2$ –, t, J = 8.0 Hz, 2H) 3.14 (–CH $_2$ –, t, J = 8.0 Hz, 2H). ^{13}C NMR (DMSO- d_6 , 300 MHz): δ 170.99, 159.01, 150.71, 149.77, 140.84, 137.32, 123.59, 122.99, 109.89, 60.48, 58.80. IR(KBr): 3334 (N–H), 1688 (C=O), 1529, 1484, 1424, 1386, 1345, 1324, 1261, 1236, 1186, 1163, 951, 828, 796, 756, 745, 696, 588 cm^{-1} . FAB MS m/z (M^+): calcd, 259.06; found, 259.27.

2.3. Preparation of 3-dipicolylamine-*N*-(quinoline-8-yl)propanamide (QP)

3-Chloro-*N*-(quinolin-8-yl)propanamide (1.17 g, 4.52 mmol), 2,2'-dipicolylamine (0.93 mL, 4.9 mmol), *N,N*-diisopropylethylamine (0.91 mL, 5.1 mmol) and potassium iodide (20 mg, 0.12 mmol) were dissolved in acetonitrile (30 mL), stirred and refluxed for 10 h under a nitrogen atmosphere. The mixture was cooled to room temperature and the solvent removed under reduced pressure to obtain a yellow oil, which was purified by silica gel column chromatography using chloroform/methanol (30:1, v/v) as eluent to afford product. Yield: 1.61 g (89.6%). 1H NMR (DMSO- d_6 , 400 MHz): δ 10.53 (NHCO, s, 1H), 8.86 (d, J = 4.0 Hz, 1H), 8.67 (d, J = 4.0 Hz, 1H), 8.45 (d, J = 4.0 Hz, 2H), 8.40 (d, J = 4.0 Hz, 1H), 7.66 (t, J = 8.0 Hz, 1H), 7.63 (t, J = 8.0 Hz, 1H), 7.55 (m, 5H) 7.16 (t, J = 8.0 Hz, 2H), 3.85 (–CH $_2$ –, s, 4H) 2.91 (–CH $_2$ –, t, J = 8.0 Hz, 2H) 2.83 (–CH $_2$ –, t, J = 8.0 Hz, 2H) ppm. ^{13}C NMR (CDCl $_3$,

Table 1
Crystallographic data for NA– $Zn(NO_3)_2$, QA– $ZnClO_4$, and QP– $ZnCl_2$.

	NA– $Zn(NO_3)_2$	QA– $ZnClO_4$	QP– $ZnCl_2$
Empirical formula	C $_{24}$ H $_{22}$ N $_6$ O $_7$ Zn	C $_{23}$ H $_{22}$ ClN $_5$ O $_6$ Zn	C $_{25}$ H $_{27}$ Cl $_2$ N $_5$ O $_2$ Zn
Formula weight	571.85	565.28	565.79
T (K)	170(2)	293(2)	170(2)293(2)
λ (Å)	0.71073	0.71073	0.71073
Space group	$P\bar{1}$	$P2_1/n$	$P\bar{1}$
a (Å)	9.0792(12)	12.3072(18)	7.5246(7)
b (Å)	10.5728(15)	13.6258(19)	9.0423(8)
c (Å)	13.6730(18)	14.514(2)	20.3129(18)
α (°)	98.742(3)	90.00	84.1570(10)
β (°)	103.224(2)	14.514(2)	87.076(2)
γ (°)	104.426(2)	90.00	65.5400(10)
V (Å 3)	1206.6(3)	2322.9(6)	1251.4(2)
Z	2	4	2
D_{calc} (Mg/m 3)	1.574	1.616	1.501
Absorption coefficient (mm $^{-1}$)	1.077	1.224	1.228
Crystal size (mm)	0.15 × 0.10 × 0.03	0.15 × 0.10 × 0.03	0.23 × 0.18 × 0.08
Reflections collected	6698	11861	6984
Independent reflections	4600 (R_{int} = 0.0243)	4420 (R_{int} = 0.1320)	4794 (R_{int} = 0.0458)
Data/restraints/parameters	4600/0/343	4420/5/329	4794/1/322
Goodness-of-fit on F^2	1.008	0.925	0.932
Final R indices [$I > 2\sigma(I)$]	R_1 = 0.0422, wR_2 = 0.0919	R_1 = 0.0793, wR_2 = 0.1985	R_1 = 0.0361, wR_2 = 0.0833
R indices (all data)	R_1 = 0.0618, wR_2 = 0.0974	R_1 = 0.1337, wR_2 = 0.2464	R_1 = 0.0468, wR_2 = 0.0856
Largest difference in peak and hole (e Å $^{-3}$)	0.545 and –0.555	0.900 and –1.578	0.514 and –0.432



Scheme 2. Synthesis of QP.

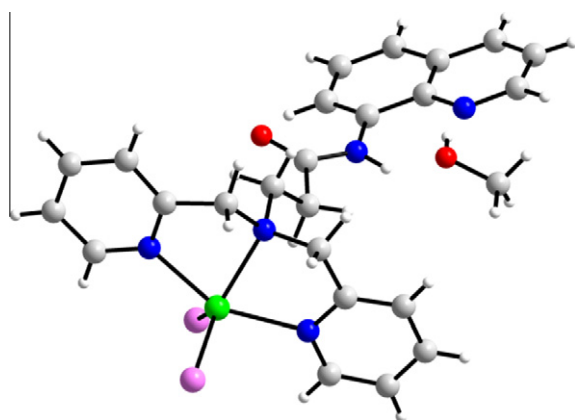


Fig. 1. Crystal structure of QP-ZnCl₂. Zn is five-coordinate, has trigonal bipyramidal geometry and does not bind the amide nitrogen or oxygen. Atom color code: Zn²⁺ green, N blue, O red, C grey, hydrogen white, and chloride pink. (For interpretation of the references to color in this figure legend, the reader is referred to the web version of this article.)

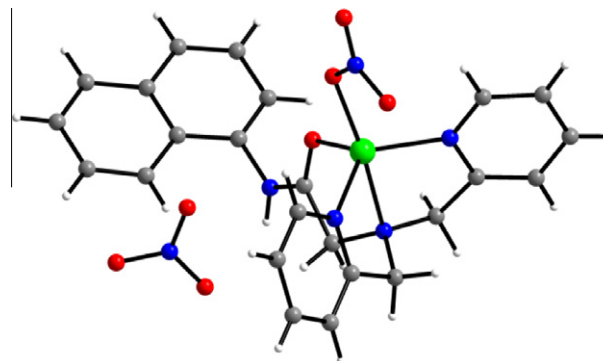


Fig. 2. Crystal structure of NA-Zn(NO₃)₂. Zn is five-coordinate and along with a nitrate group, binds nitrogens from DPA and an oxygen from the amide. Atom color code: Zn²⁺ green, N blue, O red, C grey, and hydrogen white. (For interpretation of the references to color in this figure legend, the reader is referred to the web version of this article.)

Table 2
Selected bond lengths (Å) and angles (°) for NA-Zn(NO₃)₂, QA-ZnClO₄, and QP-ZnCl₂.

NA-Zn(NO ₃) ₂			
Zn(1)–O(51)	2.007(2)	Zn(1)–N(3)	2.045(2)
Zn(1)–O(7)	2.0639(19)	Zn(1)–N(1)	2.094(3)
Zn(1)–N(2)	2.211(2)		
O(51)–Zn(1)–N(3)	105.47(9)	O(51)–Zn(1)–O(7)	92.21(8)
N(3)–Zn(1)–O(7)	112.64(9)	O(51)–Zn(1)–N(1)	106.09(10)
N(3)–Zn(1)–N(1)	120.55(9)	O(7)–Zn(1)–N(1)	114.98(9)
O(51)–Zn(1)–N(2)	170.22(8)	N(3)–Zn(1)–N(2)	79.62(9)
O(7)–Zn(1)–N(2)	78.07(8)	N(1)–Zn(1)–N(2)	77.55(9)
QA-ZnClO ₄			
N(1)–Zn(1)	2.156(6)	N(2)–Zn(1)	2.227(5)
N(3)–Zn(1)	2.172(5)	N(4)–Zn(1)	2.080(5)
N(5)–Zn(1)	2.120(5)	O(2)–Zn(1)	2.121(5)
N(4)–Zn(1)–N(5)	79.1(2)	N(4)–Zn(1)–O(2)	174.4(2)
N(5)–Zn(1)–O(2)	95.4(2)	N(4)–Zn(1)–N(1)	96.5(2)
N(5)–Zn(1)–N(1)	107.7(2)	O(2)–Zn(1)–N(1)	86.4(2)
N(4)–Zn(1)–N(3)	90.8(2)	N(5)–Zn(1)–N(3)	98.9(2)
O(2)–Zn(1)–N(3)	88.8(2)	N(1)–Zn(1)–N(3)	153.3(2)
N(4)–Zn(1)–N(2)	80.30(19)	N(5)–Zn(1)–N(2)	159.3(2)
O(2)–Zn(1)–N(2)	105.1(2)	N(1)–Zn(1)–N(2)	77.4(2)
N(3)–Zn(1)–N(2)	78.60(19)		
QP-ZnCl ₂			
Zn(1)–N(3)	2.161(2)	Zn(1)–N(1)	2.184(2)
Zn(1)–N(2)	2.233(2)	Zn(1)–Cl(1)	2.2675(8)
Zn(1)–Cl(2)	2.2744(7)		
N(3)–Zn(1)–N(1)	151.62(8)	N(3)–Zn(1)–N(2)	76.24(8)
N(1)–Zn(1)–N(2)	75.38(7)	N(3)–Zn(1)–Cl(1)	98.67(6)
N(1)–Zn(1)–Cl(1)	96.28(6)	N(2)–Zn(1)–Cl(1)	121.47(6)
N(3)–Zn(1)–Cl(2)	98.47(6)	N(1)–Zn(1)–Cl(2)	95.69(6)
N(2)–Zn(1)–Cl(2)	120.71(6)	Cl(1)–Zn(1)–Cl(2)	117.73(3)

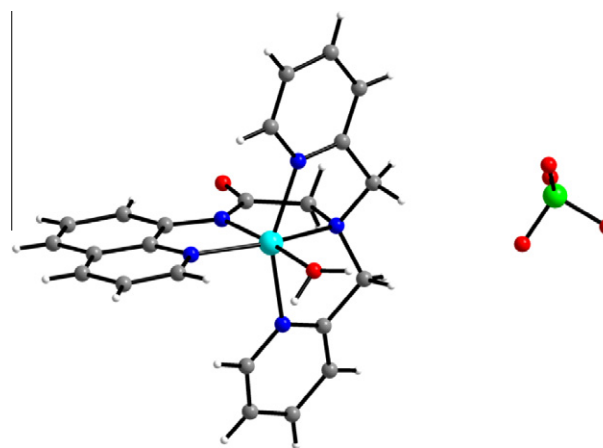


Fig. 3. Crystal structure of QA-Zn(ClO₄)(H₂O) complex. Zn²⁺ coordinates to all five nitrogens of QA. Atom color code: Zn²⁺ light blue, N blue, O red, C grey, hydrogen white, and chlorine green. (For interpretation of the references to color in this figure legend, the reader is referred to the web version of this article.)

1386.4, 1345.8, 1324.7, 1263.8, 951.3, 796.4, 756.1, 745.8, 696.1, 588.0 cm⁻¹. FAB MS *m/z* (*M*⁺): calcd, 397.47; found, 397.40. *Anal.* Calc. for C₂₄H₂₃N₅O (397.47): C, 72.52; H, 5.83; N, 17.62. Found: C, 72.50; H, 5.85; N, 17.66%.

2.4. Preparation of 2-chloro-N-(naphthalen-4-yl)acetamide

2-Chloroacetyl chloride (2.00 mL, 20.9 mmol) was dissolved in chloroform (10 mL) and added dropwise to a cooled, and stirred solution of naphthylamine (0.720 g, 5.03 mmol) and pyridine (0.43 mL, 5.2 mmol) in chloroform (10 mL) within 1 h. After the

100 MHz): δ 170.82, 148.55, 138.94, 136.30, 133.29, 128.10, 127.33, 121.82, 121.56, 116.70, 72.32, 70.70, 61.82, 53.77, 49.43 ppm. FT-IR (KBr): ν_{\max} 3334.7, 1688.1, 1529.8, 1424.3,

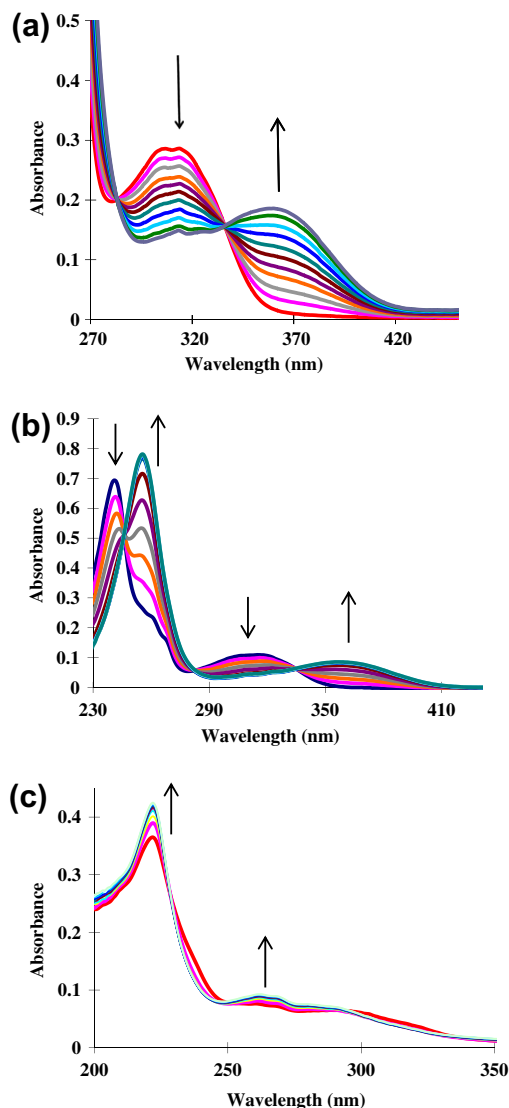


Fig. 4. UV-Vis spectra of receptors QP (a), QA (b), and NA (c) (10 μM) upon the addition of Zn²⁺ (1, 2, 3, 4, 5, 6, 7, 8, 9 and 10 μM) in Bis-tris buffer (10 mM, CH₃CN:water = 5:5 (v/v), pH = 6.5).

reaction solution was stirred for 2 h at room temperature, the solvent was removed under reduced pressure and the white powder was washed with dichloromethane and diethyl ether. Yield: 0.950 g (86.0%). Spectral characteristics matched those in the literature [17]. ¹H NMR (DMSO-*d*₆, 400 MHz): δ 10.27 (s, 1H), 8.07 (d, 1H, *J* = 9.2 Hz), 7.97 (d, 1H, *J* = 6.8 Hz), 7.82 (d, 1H, *J* = 8.0 Hz), 7.69 (d, 1H, *J* = 6.8 Hz), 7.60 (m, 3H), 4.45 (s, 2H). ¹³C-NMR (DMSO-*d*₆, 100 MHz): δ 165.4, 140.8, 134.3, 128.6, 126.0, 125.1, 124.7, 121.0, 109.4, 42.8 ppm. FT-IR (KBr): ν_{max} 3253, 1663, 1548, 1505, 1392, 1348, 1318, 1203, 1169, 1017, 960, 789 cm⁻¹. ESI-MS *m/z* (M+Na⁺): calcd, 242.04; found, 242.07.

2.5. Preparation of 2-dipicolylamine-*N*-(naphthalene-4-yl)acetamide (NA)

2-Chloro-*N*-(naphthalen-4-yl)acetamide (1.10 g, 5.01 mmol), 2,2'-dipicolylamine (0.93 mL, 4.9 mmol), *N,N*-diisopropylethylamine (0.91 mL, 5.1 mmol) and potassium iodide (20 mg) were dissolved in acetonitrile (30 mL), stirred and refluxed for 10 h under nitrogen atmosphere. The mixture was cooled to room

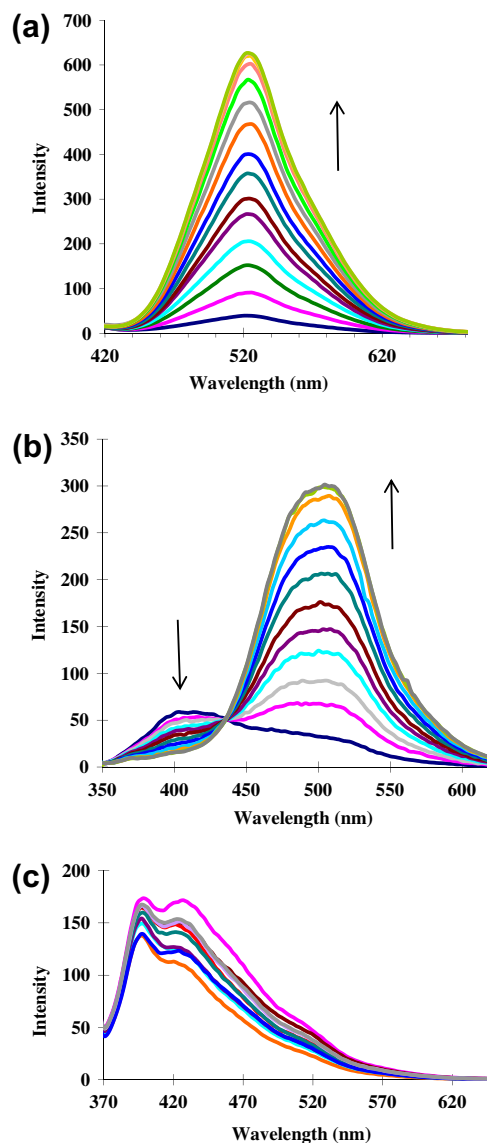


Fig. 5. Fluorescence spectra of receptor QP (a), QA (b), and NA (c) (5 μM) upon the addition of Zn²⁺ (0.5, 1.0, 1.5, 2.0, 2.5, 3.0, 3.5, 4.0, 4.5, 5.0, 5.5, 6.0, 6.5 and 7.0 μM) in a Bis-tris buffer (10 mM, CH₃CN:water = 5:5 (v/v), pH = 6.5, λ_{ex}: QP 365 nm, QA 330 nm, NA 366 nm).

temperature and the solvent was removed under reduced pressure to obtain a yellow oil, which was purified by silica gel column chromatography using chloroform/methanol (30:1, v/v) as eluent to afford product. Yield: 1.38 g (73.6%). ¹H NMR (DMSO-*d*₆, 400 MHz): δ 10.82 (s, 1H), 8.47 (d, 2H, *J* = 7.6 Hz), 8.36 (d, 1H, *J* = 4.0 Hz), 7.95 (t, 2H, *J* = 6.4 Hz), 7.77 (t, 3H, *J* = 7.6 Hz), 7.63 (t, 2H, *J* = 8.0 Hz), 7.51 (t, 3H, *J* = 8.0 Hz), 3.56 (s, 2, H) ppm. ¹³C NMR (DMSO-*d*₆, 100 MHz): δ 168.5, 156.2, 148.7, 140.8, 136.2, 134.2, 128.6, 126.6, 126.0, 124.1, 121.0, 119.0, 59.6, 56.6 ppm. FT-IR (KBr): ν_{max} 3258.38(s), 1667.28(s), 1557.79(s), 1505.58(w), 1398.9(m), 1349.43(m), 1249.6(m), 1207.6(m), 814.15(w), 793.36(m), 770.45(m) cm⁻¹. Anal. Calc. for C₂₄H₂₀N₄O (382.46): C, 75.37; H, 5.80; N, 14.65. Found: C, 75.36; H, 5.87; N, 14.74%.

2.6. X-ray crystallography

The diffraction data for compounds were collected on a Bruker SMART AXS diffractometer using Mo Kα (λ = 0.71073 Å). The crystals were mounted on a glass fiber under epoxy. The CCD data were

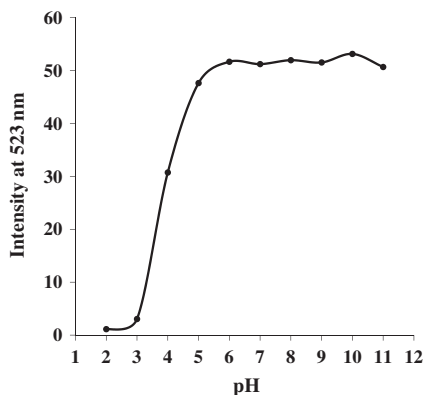


Fig. 6. Effect of the pH on the fluorescence intensity of receptor QP (5 μM) in the presence of Zn^{2+} (10 μM).

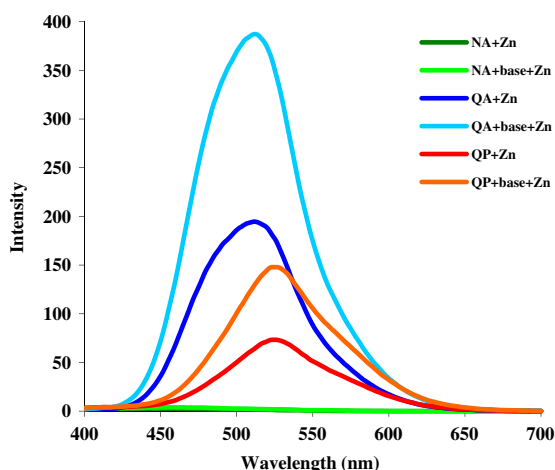


Fig. 7. Fluorescence spectra of receptors NA, QA and QP (5 μM) with Zn^{2+} (10 μM) in the absence and presence of added NH_4OH .

integrated and scaled using a Bruker SAINT, and the structures were solved and refined using SHELXTL. Hydrogen atoms were located in the calculated positions. The crystallographic data is in Table 1.

3. Results and discussion

3.1. Synthesis and crystal structures

The QP compound was synthesized by adding chloropropionyl chloride to aminoquinoline in the presence of pyridine as base (Scheme 2). After the amide bond is formed, DPA is attached to the ethyl group and QP is complete. The DPA has three zinc binding sites and the nitrogen or oxygen of the amide can act as another binding site, along with the nitrogen of the quinoline. There is a five atom distance between the amine nitrogen of DPA and the nearest coordinating atom of the fluorophore, the nitrogen or oxygen of the amide. A six-membered ring will be created when zinc coordinates to both the amine nitrogen and either the amide oxygen or nitrogen. For zinc, six membered rings are possible, but they are not as favorable as five-membered rings. Thus we propose that the QP sensor will have different binding abilities to transition metal ions than QA.

A second sensor, QA, is synthesized in a similar manner to QP, except chloroacetyl chloride is substituted for chloropropionyl chloride [16]. QA has one less CH_2 group between DPA and the

fluorophores, thus a five-membered metal–ligand ring will form when Zn^{2+} binds to the amine nitrogen of DPA and the amide oxygen or nitrogen. A third molecule, NA, was also synthesized in a similar manner to QA, but with the use of amino naphthalene in place of amino quinoline. NA is similar to QA, having only one CH_2 group between DPA and the amide, but it is also different, it having a naphthalene group instead of a quinoline group. It thus does not have a nitrogen in the fluorophore. These three compounds allow for testing the effect of an extra methylene group between DPA and the fluorophore and a nitrogen in the fluorophore.

Coordinating these three compounds to Zn^{2+} shows the ability of DPA to coordinate in different modes and the versatile coordination geometries of Zn^{2+} to sensor molecules. Crystals of QP coordinated to ZnCl_2 show planar (meridional) DPA and five coordinated Zn^{2+} in a trigonal bipyramidal geometry (Fig. 1). The DPA of the QP– ZnCl_2 complex has a $\text{N}_{\text{py}}\text{–Zn–N}_{\text{py}}$ bond angle of 151° and $\text{N}_{\text{py}}\text{–Zn–N}_{\text{amine}}$ bond angles less than 90° (76° and 75° , Table 2). The Cl–Zn–Cl bond angle is 118° and close to 120° . Surprisingly, neither the amide oxygen or nitrogen nor the nitrogen of quinoline are bound to the zinc. Thus the anions are competitive binders for Zn in polar organic environments, such as methanol from which the crystals were grown. The Zn–N_{py} bond lengths are 2.16 and 2.18 Å and the $\text{Zn–N}_{\text{amine}}$ is a little longer at 2.23 Å. These Zn–N bond lengths are very similar to other meridional DPA–Zn complexes [18]. The Zn–Cl bond lengths are not much longer than the Zn–N bond lengths and are 2.27 Å.

When NA coordinates to Zn^{2+} , it binds through the DPA nitrogens and the amide oxygen (Fig. 2). The five-coordinate Zn^{2+} also binds to an oxygen atom of a nitrate anion and resides in a trigonal bipyramidal geometry, with the amine N and nitrate O at the apexes. The $\text{N}_{\text{py}}\text{–Zn–N}_{\text{py}}$ bond angle is 120° and the $\text{N}_{\text{py}}\text{–Zn–O}_{\text{amide}}$ bond angles are slightly less at 115° and 113° . Although the $\text{N}_{\text{py}}\text{–Zn–N}_{\text{amine}}$ bond angles are 80° and 78° , the $\text{N}_{\text{py}}\text{–Zn–N}_{\text{py}}$ bond angle is 121° . Thus the DPA is clearly not in a meridional configuration, but has a facial orientation. NA bonding through the oxygen implies that it is more favorable for oxygen to bind than it is for nitrogen in methanol solvent, from which the Zn–NA complex was crystallized. Bonding through oxygen might be due to the oxygen being more basic than the nitrogen or the naphthalene group having more entropy when the oxygen is bound. The DPA is in a nearly facial arrangement on the Zn. Computer energy minimization studies show that the energy of the Zn–NA complex bonded through the amide oxygen is very similar to the Zn–NA complex bonded through the amide nitrogen. Except for the Zn–N_{am} , which is 2.21 Å, the bond lengths are shorter than they were for the Zn–QP complex. The Zn–N_{py} bond lengths are 2.05 and 2.09 Å, almost a tenth of an angstrom shorter. The shorter distance is probably an artifact of DPA not being in a meridional conformation, and thus the N's are allowed to approach the Zn more closely. The Zn–O_{am} bond length is 2.06 Å and close to the Zn–N_{py} bond lengths. The $\text{Zn–O}_{\text{nitrate}}$ is the shortest bond at 2.01 Å.

The crystal structure of QA bound to Zn shows a nearly octahedral complex with Zn bonded to all of the nitrogens of QA and a water molecule (Fig. 3). This complex was prepared by adding base during the synthesis, resulting in the amide N being deprotonated. As seen by the crystal structure, zinc is in a pseudooctahedral environment with water being the sixth ligand. The $\text{N}_{\text{py}}\text{–Zn–N}_{\text{py}}$ bond angle is 153° and the $\text{N}_{\text{py}}\text{–Zn–N}_{\text{amine}}$ bond angles are 77° and 79° , creating a planar (meridional) DPA. The $\text{N}_{\text{amine}}\text{–Zn–N}_{\text{quin}}$ bond angle is also less than 180° (159°) and the $\text{N}_{\text{amin}}\text{–Zn–N}_{\text{amide}}$ is 80° and the $\text{N}_{\text{quin}}\text{–Zn–N}_{\text{amide}}$ is 79° . Chelation of five atoms from the sensor produces a very stable complex. The structure also shows coordination through the amide nitrogen and not the oxygen. This is favored due to the bonding of Zn^{2+} to the very basic anionic amide nitrogen. Also, coordination through the oxygen would create a seven-member ring containing Zn^{2+} , amide oxygen and the quinoline

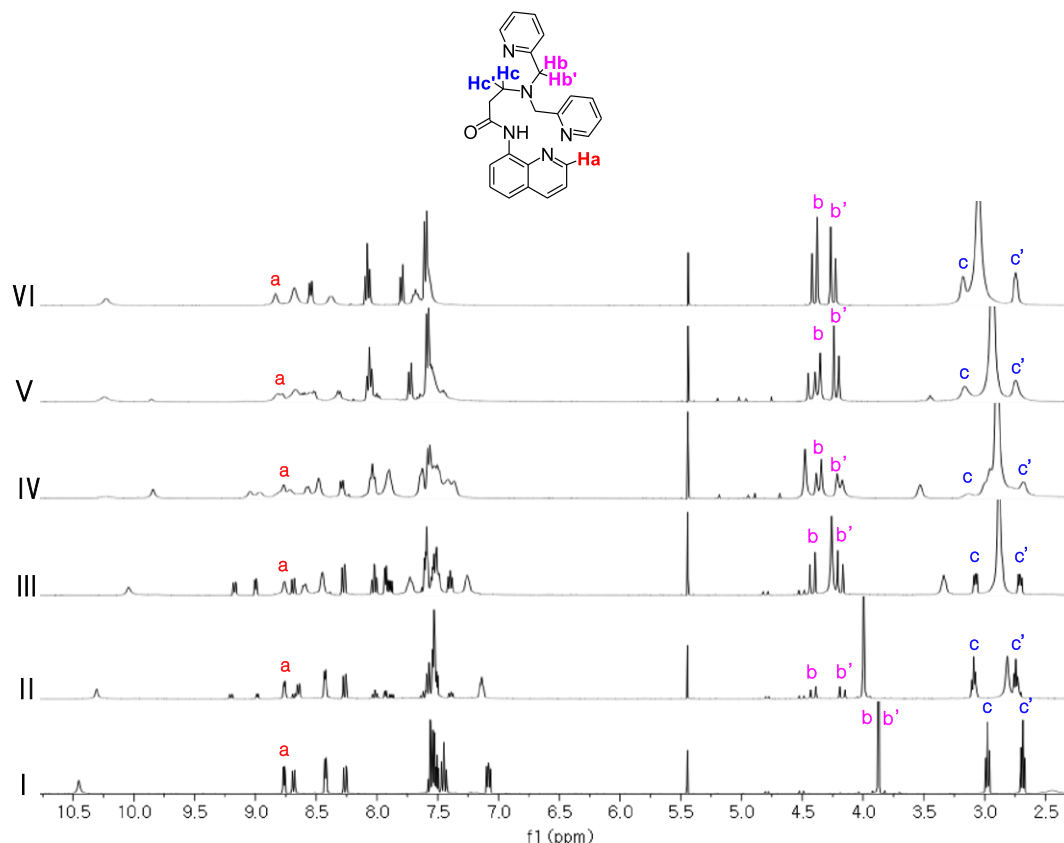


Fig. 8. ^1H NMR spectra of QP with different amounts of $\text{Zn}(\text{ClO}_4)_2$ in CD_3CN . Equivalents of Zn^{2+} : (I) 0; (II) 0.2; (III) 0.4; (IV) 0.6; (V) 0.8; (VI) 1.0.

nitrogen. The $\text{Zn}-\text{N}_{\text{amine}}$ bond length is 2.23 Å and close to what is was in the QP–Zn and NA–Zn complexes. The $\text{Zn}-\text{N}_{\text{py}}$ bond lengths are 2.16 and 2.17 Å and close to those in QP–Zn. The $\text{Zn}-\text{N}_{\text{amide}}$ bond length is the shortest at 2.08 Å. The $\text{Zn}-\text{O}_{\text{water}}$ bond length is 2.12 Å and similar to the $\text{Zn}-\text{N}_{\text{py}}$ bond lengths.

These Zn^{2+} complexes of QP, NA, and QA show the versatility of Zn coordination, it showing stable five and six coordinate complexes and octahedral and trigonal bipyramidal geometries. Several zinc salts were used to grow single crystals due to solubility and crystal growth. These crystal structures show how anions can also affect the coordination, where halides bind to zinc even in the presence of nitrogen ligands. These structures show the flexibility of the DPA ligand, which takes on meridional and facial structures as well as intermediate structures between these two extremes.

3.2. UV–Vis changes

Zinc binding to QP results in the growth of one absorbance band and the reduction of another. QP has an absorbance in the ultraviolet and one at around 310 nm. When Zn^{2+} is added to QP, a band at 370 nm grows in and the absorbance at 310 nm decreases (Fig. 4). The intensity of the 370 nm band increases up to one equivalent of Zn^{2+} and results in QP beginning to absorb in the visible light region. This increase in absorbance was seen with different solvents such as acetonitrile, water, and a mixture of acetonitrile and water. The red shift of the absorbance band of QP has also been noted in other zinc sensors [5]. The absorption enhancement at 370 nm by Zn^{2+} is also seen for Co^{2+} , but remarkably is not observed for Cd^{2+} . QA also has a peak that grows in when Zn^{2+} is added to it, but it is at 360 nm (Fig. 4). NA displays

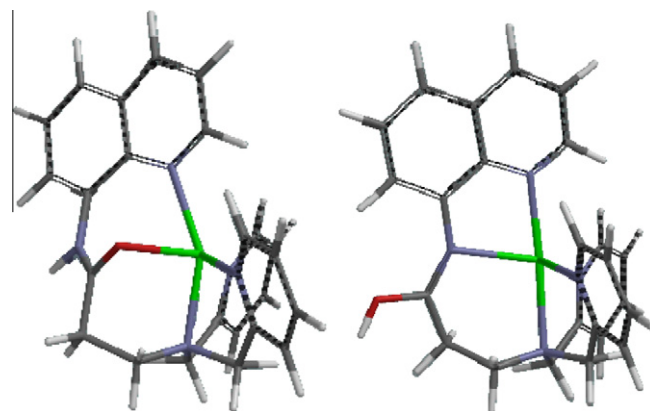


Fig. 9. Possible structures of QP binding to Zn^{2+} . Note the 7 and 6 membered rings when Zn^{2+} binds to the amide O and the 5 and 6 membered rings when Zn^{2+} binds to the amide N. Atom color code: zinc green, nitrogen blue, oxygen red, carbon grey, and hydrogen white. (For interpretation of the references to color in this figure legend, the reader is referred to the web version of this article.)

very little change in its UV–Vis signals when Zn^{2+} is added to it (Fig. 4).

3.3. Fluorescence enhancement

The fluorescence of QP is greatly enhanced by Zn^{2+} and is pH dependent. As Zn^{2+} is added to QP, the fluorescence at 525 nm increases by 10 times (Fig. 5). The percent quantum yield in acetonitrile goes from 0.29 for QP to 5.7 for the QP–Zn complex. The fluorescence increases up to one equivalent of Zn^{2+} and then levels

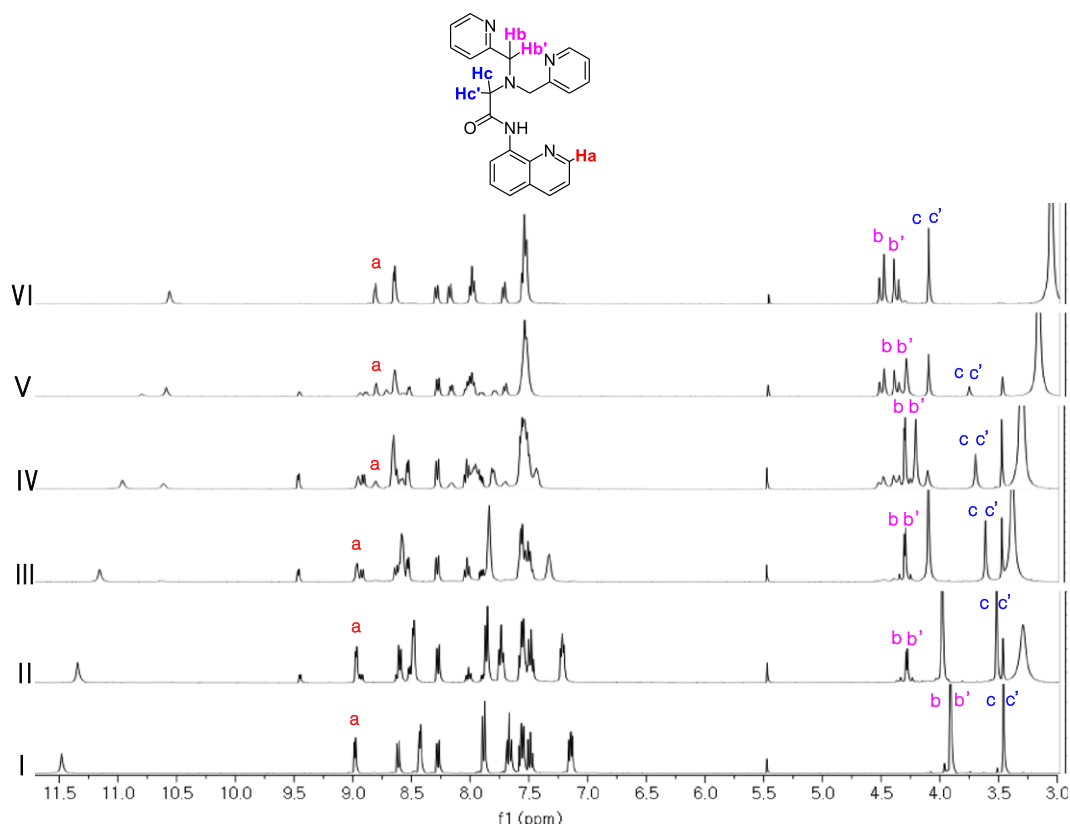


Fig. 10. ^1H NMR spectra of QA with different amounts of $\text{Zn}(\text{ClO}_4)_2$ in $\text{CD}_3\text{CN}:\text{DMSO}-d_6 = 5:5$ (v/v). Equivalents of Zn^{2+} : (I) 0; (II) 0.2; (III) 0.4; (IV) 0.6; (V) 0.8; (VI) 1.0.

off. As the equivalents of Zn^{2+} increase, the fluorescence band blue shifts by 10 nm and a shoulder at 475 nm grows in. As with the QP sensor, Zn^{2+} enhances the fluorescence of QA (Fig. 5) [16]. When Zn^{2+} is added to NA, there is very little change in fluorescence observed (Fig. 5). Thus, the nitrogen in the quinoline ring is important to fluorescence enhancement.

To gain the Zn^{2+} detection limit with QP, the equilibrium constant for QP and Zn^{2+} was found. To calculate the equilibrium constant for $\text{QP}-\text{Zn}^{2+}$, the method of Nagano et al. was used, which entailed adding QP to a HEPES buffer solution of Zn^{2+} and nitrilotriacetic acid [19]. Fluorescence changes were monitored under these conditions and used to calculate an apparent dissociation constant of 0.024 nM. Thus QP binds Zn^{2+} very strongly, as expected due to its DPA and amide groups and Zn^{2+} detection limits for QP could be in the sub nanomolar range. The dissociation constant for QP is similar to QA and those of other sensors [4,11,16].

The enhanced fluorescence of QP by Zn^{2+} is small at low pH, raises from 2 to 6, and reaches a maximum at 6, where it plateaus until the pH is above 10 (Fig. 6). This pH range is good for imaging Zn^{2+} at around pH 7 and in biological media. At low pH, Zn^{2+} and H^+ are competing for the nitrogen sites of QP and Zn^{2+} does not bind strongly. As the pH increases and the H^+ concentration decreases, Zn^{2+} binds more strongly to QP and enhances fluorescence.

While using QA, we also noted that the Zn^{2+} enhanced fluorescence of QA can be doubled if the amide proton of QA is removed (Fig. 7). When base is added to QA and the $[\text{QA}^--\text{Zn}]^+$ complex is formed ($\Phi = 0.15$), the fluorescence is much greater than it is for QA ($\Phi = 0.002$), QA^- ($\Phi = 0.023$) and $[\text{QA}-\text{Zn}]^{2+}$ ($\Phi = 0.078$). This remarkable fluorescence enhancement due to deprotonation is not observed to such a great extent for QP (QP $\Phi = 0.003$, QP^- $\Phi = 0.004$, $[\text{QP}-\text{Zn}]^{2+}$ $\Phi = 0.057$, $[\text{QP}^--\text{Zn}]^+$ $\Phi = 0.061$). The enhanced fluorescence of QA can be explained by stronger binding

of the amide N to Zn^{2+} due to its anionic nature and thus rendering the electrons of the N less able to be involved in photo-induced electron transfer (PET). It could also be due to the lowering of the energy of the amide N orbital which contains the lone pair of electrons and thus making it more energetically unfavorable for them to participate in PET.

3.4. NMR characterization

It is evident by the proton chemical shift changes that Zn^{2+} binds to QP. The methylene protons of DPA move downfield and split into doublets as soon as Zn^{2+} is added, whether the solvent is acetonitrile, DMSO, methanol, or acetonitrile/water (Fig. 8). The doublet formation is characteristic of facial DPA coordination to Zn^{2+} . In DMSO, the N–H proton moves slightly downfield and in acetonitrile it moves slightly upfield, implying Zn^{2+} coordination through the amide N. In acetonitrile, however, the N–H proton moves upfield by 0.5 ppm before returning to a chemical shift close to its original position. Since the UV–Vis data show a nice isosbestic point, we propose that the proton shifts are for one or more intermediates that have the same UV–Vis absorbance. There is a great energy difference to bind through the amide N instead of the O. Binding through the amide N results in ligand–metal coordination rings of five- and six-membered, both of which are common for coordination compounds (Fig. 9). In contrast, binding through the amide O creates seven- and six-membered rings, which seven membered rings are not favorable. A computer calculation shows that binding through the N is over one hundred kJ/mol lower in energy than binding through the O.

When the ZnCl_2 salt is used in place of $\text{Zn}(\text{ClO}_4)_2$, Zn binding occurs in a different manner. After one equivalent of Zn^{2+} has been added, the methylene protons of DPA are still a singlet, implying

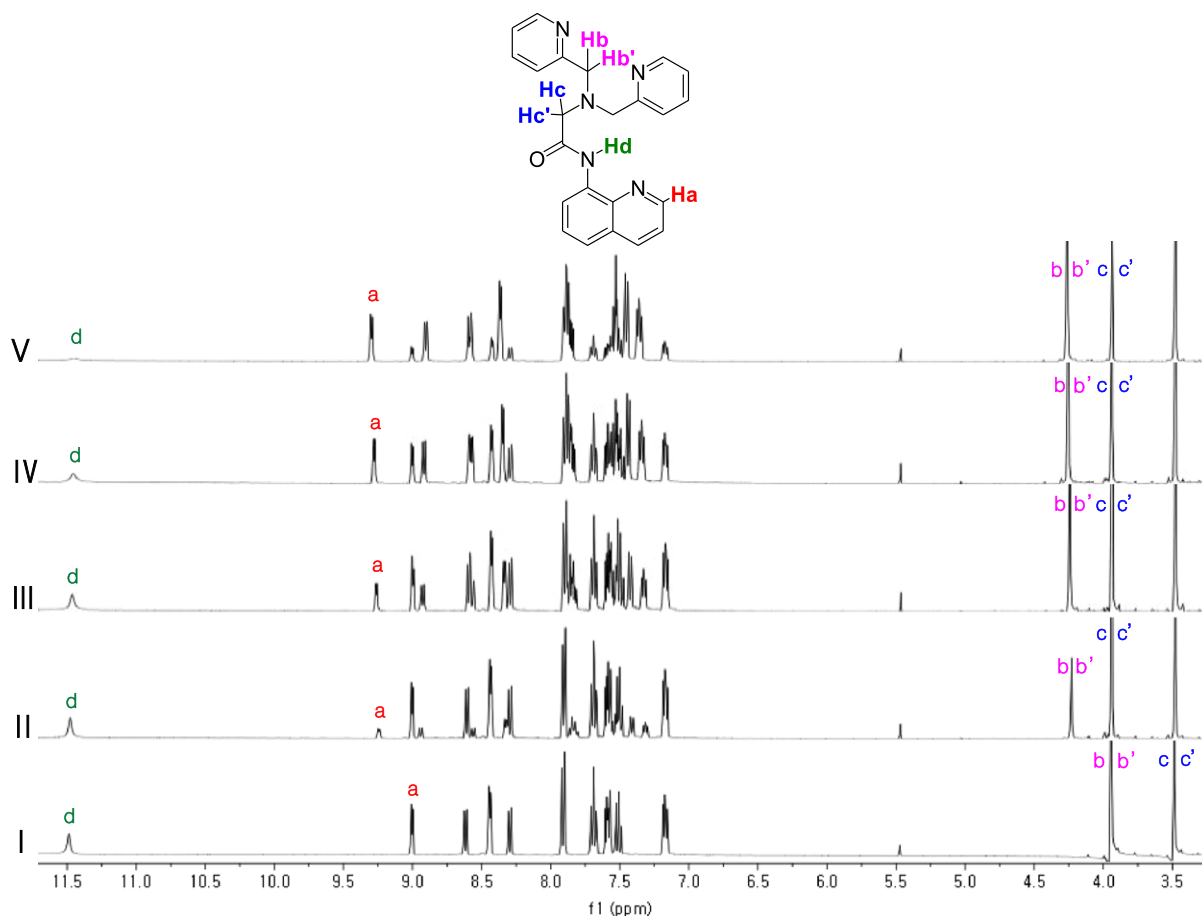


Fig. 11. ^1H NMR spectra of QA with different amounts of $\text{Zn}(\text{ClO}_4)_2$ in the presence of NH_4OH in $\text{CD}_3\text{CN}:\text{DMSO}-d_6 = 95:5$ (v/v). Equivalents of Zn^{2+} : (I) 0; (II) 0.2; (III) 0.4; (IV) 0.6; (V) 0.8.

meridional coordination of DPA as seen in the crystal structure. It requires over 2 equivalents of Zn^{2+} before the methylene protons split into doublets and for the DPA to bind facially. Whether in DMSO or acetonitrile, the amide N–H proton shifts upfield by 0.4 and 0.8 ppm, respectively. This implies Zn^{2+} binds through the carbonyl oxygen. The quinoline protons do not shift downfield, unlike the aromatic DPA protons, thus, it looks like the nitrogen in quinoline does not bind to Zn^{2+} , as seen in the crystal structure.

NMR proton chemical shifts show QA binds Zn^{2+} . Whether the solvent is acetonitrile, DMSO, or methanol the methylene protons of DPA split into doublets of doublets, implying facial coordination of DPA (Fig. 10). The DPA aromatic protons move slightly downfield as more Zn^{2+} is added. Again in all of the solvents listed above, the proton on the ortho carbon next to the N of quinoline moves downfield as Zn^{2+} is added and then goes back upfield to a position close to where it started. This implies that the quinoline is binding to Zn^{2+} and as more Zn^{2+} is added, its proton is being less deshielded. The amide N–H proton moves a large distance upfield when QA is in DMSO or acetonitrile, 0.6 and 0.9 ppm, respectively. In other compounds that have DPA linked to amides, a large change in chemical shift of the amide N–H hydrogen implies that Zn^{2+} is binding to O [5]. We don't think this is the case with QA. The increase in absorption and fluorescence of QA due to Zn^{2+} , which has a quinoline N, is much greater than what is observed for NA, which doesn't have a quinoline N. Thus, Zn^{2+} is binding to the quinoline N. If this is the case, then Zn^{2+} binding also through the amide N, creates a much more stable structure than if it were to bind through the amide O. It creates two five-membered ligand–metal

rings, instead of five- and seven-membered rings. As with QP, computer calculations show that Zn^{2+} binding to N creates a structure that is over 100 kJ/mol lower in energy.

When base is present with QA and Zn^{2+} is added, the N–H proton signal decreases upon addition of Zn^{2+} and the proton is removed by the base (Fig. 11). The DPA methylene protons 5 and 6 move downfield due to the cationic and electron withdrawing nature of Zn^{2+} . Protons 5 are a singlet, meaning DPA is meridional as seen in the crystal structure. Some of the aromatic protons on DPA also move downfield. Aromatic protons of the quinoline also move downfield, specifically, proton 8 on the ortho carbon next to the quinoline N moves 0.3 ppm downfield and the proton on the para carbon to the N of the quinoline moves 0.3 ppm downfield. Indeed, the ^1H NMR of the $[\text{QA}^--\text{Zn}]^+$ complex in DMSO has the proton 8 signal 0.5 ppm downfield. This substantial movement downfield implies the N of the quinoline ring is binding to Zn^{2+} , as seen in the crystal structure.

NA also binds Zn^{2+} as shown by changes in the proton NMR signals. In acetonitrile and methanol, the methylene protons of DPA shift and remain a broad singlet until the last partial equivalent of Zn^{2+} is added, at which point they form a doublet of doublets (Fig. 12). This is different for DMSO, where the DPA methylene protons shift downfield and begin to form a doublet of doublets after the initial Zn^{2+} is added. This implies that in acetonitrile and methanol, DPA binds meridionally and then switches to facial, while in DMSO it binds facially at the beginning. The N–H shifts slightly downfield in DMSO and slightly upfield in acetonitrile, potentially indicating Zn^{2+} binds to the amide N. This is in contrast to what is

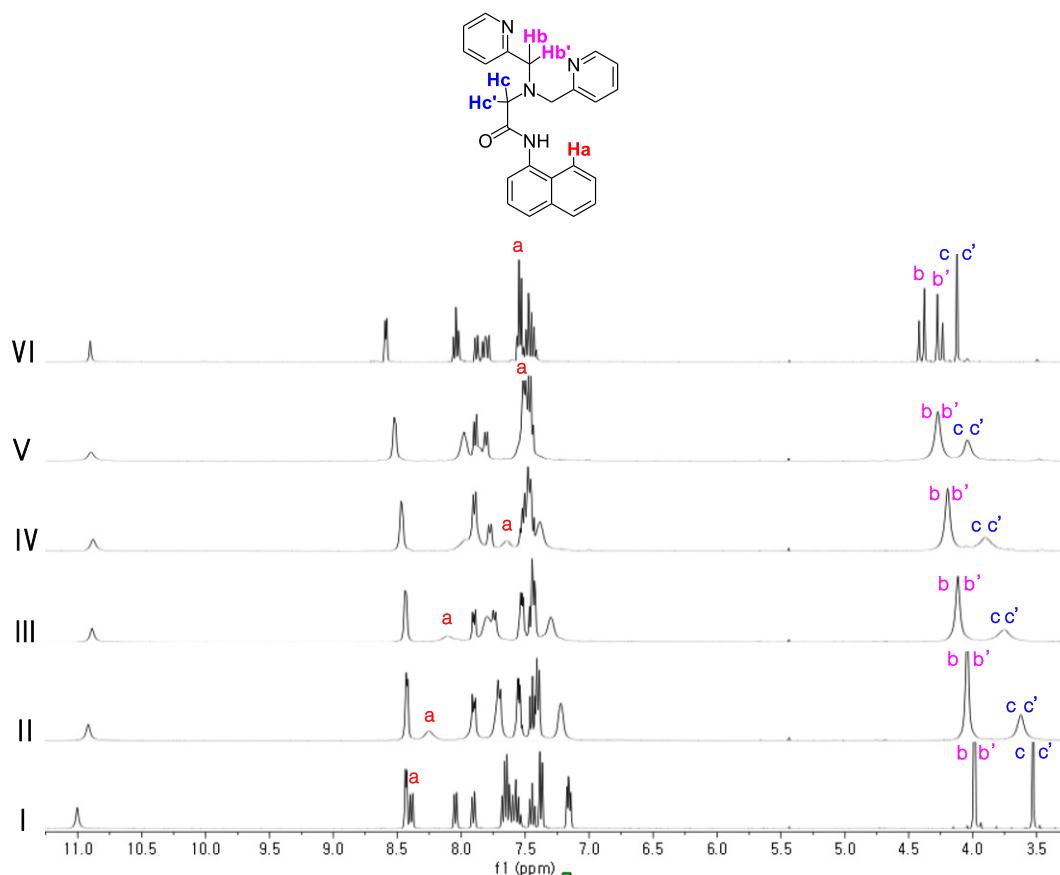


Fig. 12. ^1H NMR spectra of NA with different amounts of $\text{Zn}(\text{ClO}_4)_2$ in CD_3CN . Equivalents of Zn^{2+} : (I) 0; (II) 0.2; (III) 0.4; (IV) 0.6; (V) 0.8; (VI) 1.0.

seen in the crystal structure of the Zn–NA complex, which shows Zn bonded through the amide O. The crystals were grown in methanol, which might be why binding through the amide O is favored. We cannot track the N–H proton by NMR in methanol due to deuterium exchange, so we do not know whether it moves upfield significantly.

3.5. Selectivity

Fluorescence selectivity is critical for a Zn^{2+} sensor and QP shows high Zn^{2+} selectivity. Unlike when Zn^{2+} is added to QP and enormous fluorescence enhancement is seen, when metal ions ranging from alkali and alkaline earth (Li^+ , Na^+ , K^+ , Mg^{2+} , Ca^{2+}) to first row transition metals (Cr^{2+} , Mn^{2+} , Fe^{2+} , Co^{2+} , Ni^{2+} , Cu^{2+}) to second and third row transition metals (Cd^{2+} , Ag^+ , Hg^{2+}) are added to QP in acetonitrile it does not fluoresce (Fig. 13). When a mixture of acetonitrile/water or pure water is used, Zn^{2+} still causes the most fluorescence enhancement of QP. Remarkably, this selectivity by QP to not fluoresce in the presence of Cd^{2+} is not seen for QA, which fluoresces when Cd^{2+} is present [16]. As was noted by the absorption studies, Cd^{2+} did not cause changes to the absorption of QP. Cd^{2+} most likely doesn't bind to the amide nitrogen or oxygen and thus doesn't stop the PET process.

The fluorescence of QP is enhanced by Zn^{2+} even when other metal ions are present. In acetonitrile, Zn^{2+} enhanced fluorescence is seen when other metal ions are present, except for high concentrations of Cu^{2+} , Fe^{2+} , and Co^{2+} (Fig. 14). In a mixture of acetonitrile and water or pure water, the fluorescence of QP is greatly enhanced, except again when high equivalents of Cu^{2+} or Co^{2+} are present. This notable selectivity for Zn^{2+} is most likely due to the strong binding of Zn^{2+} to DPA and the amide group. Cu^{2+} , which

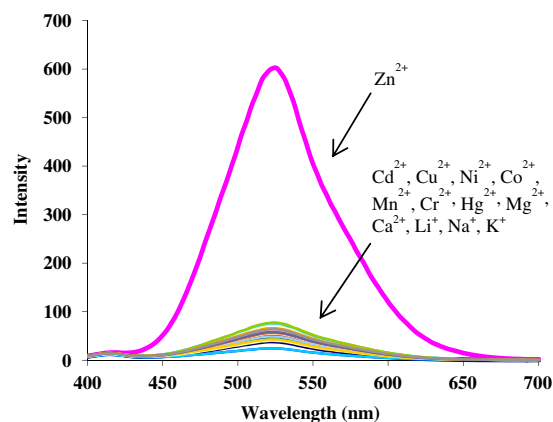


Fig. 13. Fluorescence spectra of receptor QP ($5\ \mu\text{M}$) upon the addition of different metal ions (2 equiv) in a Bis-tris buffer [10 mM, $\text{CH}_3\text{CN}:\text{water} = 5:5$ (v/v)]. Fluorescence of Zn^{2+} with QP is shown in pink. The fluorescence as a result of the other metal ions including Cd^{2+} , Cu^{2+} , Ni^{2+} , Co^{2+} , Fe^{2+} , Mn^{2+} , Cr^{2+} , Hg^{2+} , Ag^+ , Mg^{2+} , Ca^{2+} , Li^+ , Na^+ , and K^+ are the other colors. (For interpretation of the references to color in this figure legend, the reader is referred to the web version of this article.)

rivals the Lewis acidity of Zn^{2+} , is competitive for binding to QP. Also, the ability of Zn^{2+} to be stable in various geometries such as trigonal bipyramidal and octahedral, renders it a strong binding ion.

4. Conclusion

The new sensor QP shows enhanced fluorescence in the presence of Zn^{2+} . The nitrogen in the quinoline ring is important to

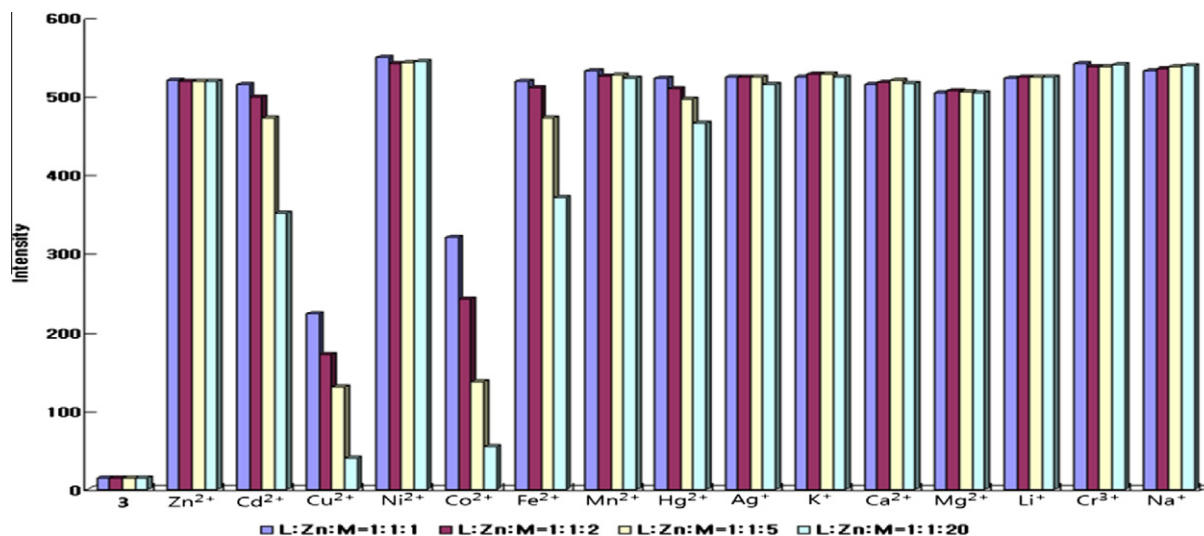


Fig. 14. Competitive selectivity of receptor QP (5 μM) toward Zn^{2+} ions (5 μM) in the presence of other metal ions (5 μM M^{n+} blue, 10 μM M^{n+} red, 25 μM M^{n+} yellow, and 100 μM M^{n+} green). (For interpretation of the references to color in this figure legend, the reader is referred to the web version of this article.)

fluorescence enhancement. QP shows selective fluorescence for Zn^{2+} and not for other transition metal ions. The DPA group of zinc sensors is able to conform to different structures from meridional to facial. The fluorescence enhancement of Zn^{2+} binding to QA is greatly enhanced by adding base. The ^1H NMR chemical shift changes of QP, QA, and NA when Zn^{2+} binds to them show the type of DPA binding.

Acknowledgments

Financial support from Korean Science & Engineering Foundation (2009-0074066), Converging Research Center Program through the National Research Foundation of Korea (NRF) funded by the Ministry of Education, Science and Technology (2009-0082832), and Brigham Young University is gratefully acknowledged.

Appendix A. Supplementary material

CCDC 867079, 867080 and 867081 contain the supplementary crystallographic data for complexes $\text{NA-Zn}(\text{NO}_3)_2$, QA-ZnClO_4 and QP-ZnCl_2 , respectively. These data can be obtained free of charge from The Cambridge Crystallographic Data Centre via http://www.ccdc.cam.ac.uk/data_request/cif. Supplementary data associated with this article can be found, in the online version, at <http://dx.doi.org/10.1016/j.ica.2012.09.009>.

References

- [1] (a) N.C. Lim, H.C. Freake, C. Brückner, *Chem. Eur. J.* 11 (2005) 38; (b) Z. Dai, J.W. Canary, *New J. Chem.* 31 (2007) 1708; (c) E.L. Que, W. Eomaille, C.J. Chang, *Chem. Rev.* 108 (2008) 1517; (d) E. Tomat, S.J. Lippard, *Curr. Opin. Chem. Biol.* 14 (2010) 225.
- [2] (a) L.E. McQuade, S.J. Lippard, *Inorg. Chem.* 49 (2010) 9535; (b) B.A. Smith, W.J. Akers, W.M. Leevy, A.J. Lampkins, S. Xiao, W. Wolter, M.A. Suckow, S. Achilefu, B.D. Smith, *J. Am. Chem. Soc.* 132 (2010) 67; (c) Z. Xu, K.-H. Baek, H.N. Kim, J. Cui, X. Qian, D.R. Spring, I. Shin, J. Yoon, *J. Am. Chem. Soc.* 132 (2010) 601; (d) E.M. Nolan, S.J. Lippard, *Acc. Chem. Res.* 42 (2009) 193; (e) Y. Mei, C.J. Frederickson, L.J. Gibling, J.H. Weiss, Y. Medvedeva, P.A. Bentley, *Chem. Commun.* 47 (2011) 7107.
- [3] A.P. de Silva, H.Q.N. Gunaratne, T. Gunnlaugsson, A.J.M. Huxley, C.P. McCoy, J.T. Rademacher, T.E. Rice, *Chem. Rev.* 97 (1997) 1515.
- [4] (a) C.R. Goldsmith, S.J. Lippard, *Inorg. Chem.* 45 (2006) 555; (b) K. Kiyose, H. Kojima, Y. Urano, T. Nagano, *J. Am. Chem. Soc.* 128 (2006) 6548; (c) J. Meeusen, H. Tomasiewicz, A. Nowakowski, D.H. Petering, *Inorg. Chem.* 50 (2011) 7563; (d) X.-B. Yang, B.-X. Yang, J.-F. Ge, Y.-J. Xu, Q.-F. Xu, J. Liang, J.-M. Lu, *Org. Lett.* 13 (2011) 2710; (e) P. Das, S. Bhattacharya, S. Mishra, A. Das, *Chem. Commun.* 47 (2011) 8118; (f) A.E. Lee, M.R. Grace, A.G. Meyer, K.L. Tuck, *Tetrahedron Lett.* 51 (2010) 1161; (g) Z. Liu, C. Zhang, Y. Li, Z. Wu, F. Qian, X. Yang, W. He, X. Gao, Z. Guo, *Org. Lett.* 11 (2009) 795.
- [5] (a) Z. Xu, K.-H. Baek, H.N. Kim, J. Cui, X. Qian, D.R. Spring, I. Shin, J. Yoon, *J. Am. Chem. Soc.* 132 (2010) 601; (b) H.G. Lee, J.H. Lee, S.P. Jang, H.M. Park, S.-J. Kim, Y. Kim, C. Kim, R.G. Harrison, *Tetrahedron* 67 (2011) 8073.
- [6] C.J. Fahrni, T.V. O'Halloran, *J. Am. Chem. Soc.* 121 (1999) 11448.
- [7] Y. Zhang, X. Guo, W. Si, L. Jia, X. Qian, *Org. Lett.* 10 (2008) 473.
- [8] X. Zhou, B. Yu, Y. Guo, X. Tang, H. Zhang, W. Liu, *Inorg. Chem.* 49 (2010) 4002.
- [9] (a) C. Núñez, R. Bastida, A. Macías, E. Bértolo, L. Fernandes, J.L. Capelo, C. Lodeiro, *Tetrahedron* 65 (2009) 6179; (b) M. Marni, M.C. Aragoni, M. Arca, M. Atzori, A. Bencini, C. Bazzicalupi, A.J. Blake, C. Caltagirone, F.A. Devillanova, A. Garau, M.B. Hursthouse, F. Isaia, V. Lippolis, B. Valtancoli, *Inorg. Chem.* 48 (2009) 9236; (c) J. Jiang, T. Xiaoliang, L. Yang, W. Dou, W. Liu, R. Fang, W. Liu, *Dalton Trans.* 40 (2011) 6367; (d) I. Ravikumar, P. Ghosh, *Inorg. Chem.* 50 (2011) 4229.
- [10] J.-F. Zhu, H. Yuan, W.-H. Chan, A.W.M. Lee, *Tetrahedron Lett.* 51 (2010) 3550.
- [11] H.-H. Wang, Q. Gan, X.-J. Wang, L. Xue, S.-H. Liu, H. Jiang, *Org. Lett.* 9 (2007) 4995.
- [12] L. Xue, C. Liu, H. Jiang, *Chem. Commun.* (2009) 1061.
- [13] X.-Y. Chen, J. Shi, Y.-M. Li, F.L. Wang, X. Wu, Q.X. Guo, L. Liu, *Org. Lett.* 11 (2009) 4426.
- [14] L. Xue, Q. Liu, H. Jiang, *Org. Lett.* 11 (2009) 3454.
- [15] Y. Mikata, A. Yamashita, K. Kawata, H. Konno, S. Itami, K. Yasuda, S. Tamotsu, *Dalton Trans.* 40 (2011) 4059.
- [16] J. Du, J. Fan, X. Peng, H. Li, S. Sun, *Sens. Actuators B: Chem.* 144 (2010) 337.
- [17] S.E. Plush, N.A. Clear, J.P. Leonard, A.-M. Fanning, T. Gunnlaugsson, *Dalton Trans.* 3 (9) (2010) 3644.
- [18] (a) B.K. Park, S.H. Lee, E.Y. Lee, H. Kwak, Y.M. Lee, Y.J. Lee, J.Y. Jun, C. Kim, S.J. Kim, Y. Kim, *J. Mol. Struct.* 890 (2008) 123; (b) Y. Kim, B.K. Park, G.H. Eom, S.H. Kim, H.M. Park, Y.S. Choi, H.G. Jang, C. Kim, *Inorg. Chim. Acta* 366 (2011) 337.
- [19] S. Maruyama, K. Kikuchi, T. Hirano, Y. Urano, T. Nagano, *J. Am. Chem. Soc.* 124 (2002) 10650.